

See discussions, stats, and author profiles for this publication at:  
<https://www.researchgate.net/publication/257346182>

# Infrared and Raman spectra of $^{12}/^{13}\text{C}$ -thallium nitroprusside, $\text{Tl}_2[\text{Fe}(\text{CN})_5\text{NO}]$

ARTICLE in VIBRATIONAL SPECTROSCOPY · APRIL 2000

Impact Factor: 2 · DOI: 10.1016/S0924-2031(99)00075-2

---

READS

25

3 AUTHORS, INCLUDING:



**Elizabeth Chacón Villalba**

National University of La Plata

17 PUBLICATIONS 136 CITATIONS

SEE PROFILE



**Eduardo L. Varetti**

Facultad de Ciencias Exactas, Universi...

125 PUBLICATIONS 1,130 CITATIONS

SEE PROFILE

# Infrared and Raman spectra of $^{12/13}\text{C}$ -thallium nitroprusside, $\text{Ti}_2[\text{Fe}(\text{CN})_5\text{NO}]$

M.E. Chacón Villalba<sup>1</sup>, E.L. Varetti<sup>2</sup>, P.J. Aymonino<sup>\*,2</sup>

CEQUINOR, Centro de Química Inorgánica (CONICET, UNLP) and LANAIS EFO, Laboratorio Nacional de Investigación y Servicios en Espectrofotometría Óptica (CONICET-UNLP), Departamento de Química, Facultad de Ciencias Exactas, Universidad Nacional de La Plata, 47 esq. 115, C. Correo 962, 1900 La Plata, Argentina

Received 22 January 1999; received in revised form 7 September 1999; accepted 27 September 1999

## Abstract

Interferometric infrared and Raman spectra of thallium nitroprusside ( $\text{Ti}_2[\text{Fe}(\text{CN})_5\text{NO}]$ ), with normal isotopic composition or substituted with  $^{13}\text{C}$  (98.5%), were obtained from 4000 to 50  $\text{cm}^{-1}$  at room and low temperature (boiling liquid air). Infrared microscopy used with selected monocrystals allowed the detection of very weak overtone and combination bands. Comparisons are made with other nitroprusside salts, anhydrous and hydrated, and especially with sodium nitroprusside dihydrate. © 2000 Elsevier Science B.V. All rights reserved.

**Keywords:** Infrared; Raman; Thallium nitroprusside;  $^{13}\text{C}$ -nitroprusside; Isotopic replacement

## 1. Introduction

The structural and vibrational properties of a series of crystalline, generally hydrated, nitroprussides have been studied in this laboratory, including alkaline [1–6], alkaline earth [7–10] and transition metal [11] salts. Only the alkaline nitroprussides having the larger cations, namely Rb and Cs (RbNP and CsNP) crystallize as anhydrous compounds [5,6]. Such anhydrous compounds are useful to identify bands due to the internal vibrations of the anion in hydrated nitroprussides in which the presence of libration

water bands makes difficult a proper band assignment, mainly below 700  $\text{cm}^{-1}$ . However, CsNP is less useful for that purpose because two crystallographic different anions exist in the lattice. We found that more useful are RbNP and the Tl salt (TINP), in both of which the anions are in sites of  $C_1$  symmetry [5,12], lifting up the degeneracy of the E modes, whose bands appear therefore as doublets facilitating a proper vibrational assignment. Such splitting is much more defined in TINP than in RbNP (in which the splitting of some bands is visible only at low temperature). In fact, the infrared spectra of TINP was used as a term of comparison to define the assignment of the bands associated with the E modes in a quantum chemistry determination of the nitroprusside force field taking as a basis the available experimental data for the dehydrated sodium salt, NaNP [13].

\* Corresponding author. Tel.: +54-221-4214037; fax: +54-221-1259485; e-mail: aymonino@dalton.quimica.unlp.edu.ar

<sup>1</sup> Assistant Member of the Professional Research Career, CI-CPBA, R. Argentina.

<sup>2</sup> Member of the Research Career, CONICET, R. Argentina.

The NIR spectra of TINP has been used also to improve the assignment of overtone and combination bands in NaNP, in which the water bands also complicate the 8000–4000  $\text{cm}^{-1}$  region [14].

We report now the infrared and Raman spectra of TINP in its normal and  $^{13}\text{C}$  substituted forms and at room and low temperatures. The assignment of bands to the different normal modes of vibration is based in the previous theoretical calculations [13].

## 2. Experimental

### 2.1. Preparative

Stoichiometric quantities of 0.015 M aqueous solutions of sodium nitroprusside (Merck, p.a.) and 0.015 M silver nitrate were mixed under stirring and the pink precipitate obtained was added, after separation by filtration, to a stoichiometric quantity of 0.015 M barium chloride aqueous solution, maintaining the mixture under vigorous agitation during 3 h. To the solution of barium nitroprusside so obtained, separated from the solid by centrifugation, a stoichiometric amount of a 0.015-M aqueous  $\text{Ti}_2\text{SO}_4$  solution was added with stirring and the barium sulfate formed was separated by centrifugation; anhydrous TINP was obtained as very small crystals by concentration of the solution at room temperature [15].

$^{13}\text{C}$ -nitroprusside was previously obtained as the sodium salt from  $\text{Na}^{13}\text{CN}$  (98.5%, Merck, Sharp & Dohme) as in Ref. [2] and the product was used to prepare the thallium salt following the above indicated procedure.

### 2.2. Infrared and Raman spectra

The following Bruker FTIR spectrophotometers were used: (a) IFS 113v provided with an Oxford OX8 ITL cryostat and (b) IFS 66 with IR microscope A590 and Raman module FRA106.

Medium infrared (4000 to 300  $\text{cm}^{-1}$ ) spectra were measured with samples mulled in Nujol and spread between CsI windows (ion exchange was observed in NaBr and KBr pellets) whereas far infrared spectra (300 to 50  $\text{cm}^{-1}$ ) were obtained with polyethylene pellets. The spectral region com-

prised between 10000 and 700  $\text{cm}^{-1}$  was searched for overtones and combination bands with the infrared microscope and single crystals of adequate thickness or using very thick Nujol mulls. Raman spectra were obtained with powdered samples using light of 1064 nm from a Nd/YAG laser for excitation.

## 3. Crystal and anion structures and anion internal vibrational modes

TINP crystallizes in the monoclinic  $C_c$  ( $C_s^4$ )  $N^\circ 9$  space group,  $Z = 4$  [12]. The anion occupies a set of four  $C_1$  sites and is a distorted octahedron, with the four CN equatorial groups slightly bent towards the fifth, axial CN group. The NO group is opposite to this CN group and is also slightly bent.

The simplest, ideal symmetry of the anion should be  $C_{4v}$ , with a linear  $(\text{CN})_{\text{ax}}$  FeNO moiety and geometrically equivalent  $(\text{CN})_{\text{eq}}$  groups. Thirty-three internal modes of vibration are expected for the isolated anion of  $C_{4v}$  symmetry and are represented as follows:  $\Gamma(C_{4v})$ :  $8A_1(\text{IR}, \text{R}) + 1A_2$  (inactive) +  $4B_1(\text{R}) + 2B_2(\text{R}) + 9E(\text{IR}, \text{R})$ . For the anion in the crystal site ( $C_1$ ), the representation of the vibrations is the following:  $\Gamma(C_1)$ :  $33A$  (IR, R). The representation of the 66 internal vibrational modes of the primitive unit cell ( $Z = 2$ ) is:  $\Gamma(C_s)$ :  $33 A'(\text{IR}, \text{R}) + 33 A''(\text{IR}, \text{R})$ .

## 4. Bands assigned to fundamental modes

Table 1 collects infrared and Raman wavenumbers for isotopically normal ( $^{12}\text{C}$  98.9% natural abundance) and  $^{13}\text{C}$ -substituted (98.5% isotopic purity) TINP. Measured and calculated isotopic shifts are also included in the table. Assignments follow the results of a quantum chemistry vibrational study of the anion in NaNP [13], as said before.

Figs. 1 and 2 reproduce room and low temperature infrared spectra and room temperature Raman spectra. The inserts show expanded the regions where the stretching bands of isolated CN and NO groups appear (see below). Intensities of bands in the 700–100  $\text{cm}^{-1}$  region (Fig. 2) are increased with respect to the region above 700  $\text{cm}^{-1}$  for the sake of clarity.

Table 1

Infrared and Raman wavenumbers and isotopic shifts of  $^{12/13}\text{C-Tl}_2[\text{Fe}(\text{CN})_5\text{NO}]$  at room and low temperatures

Symmetry species <sup>a</sup>	Assignment <sup>b</sup>	Infrared <sup>c</sup>				Raman		$\Delta_i^{12/13}\text{C}^{\text{c,d}}$			$\Delta_i^{12/13}\text{C}$ calculated <sup>e</sup>
		$^{12}\text{C}$ r.t.	$^{12}\text{C}$ l.t.	$^{13}\text{C}$ r.t.	$^{13}\text{C}$ l.t.	$^{12}\text{C}$	$^{13}\text{C}$	IR r.t.	IR l.t.	Raman	
A <sub>1</sub>	$\nu\text{CN}_{\text{ax}}$	2146	2150	2100	2103	2147	2101	47	47	46	47.7
A <sub>1</sub>	$\nu\text{CN}_{\text{eq}}$	2140	2142	2093	2095	2141	2094	47	47	47	47.6
B <sub>1</sub>	$\nu\text{CN}_{\text{eq}}$	2134	2135	2087	2089	2135	2088	47	46	47	47.4
E	$\nu\text{CN}_{\text{eq}}$	2122	2123	2076	2078	2124	2078	46	45	46	46.9
A <sub>1</sub>	$\nu\text{NO}$	1947	1948	1945	1952	–	–	2	4	–	0.4
E	$\delta\text{FeNO}$	660/658	663/660	658/655	661/658	660	659/655	2/3	2/2	3	2.6
A <sub>1</sub>	$\nu\text{FeN}$	643	646	641	644	644	642	2	2	2	2.7
E	$\nu\text{FeC}_{\text{eq}}, \delta\text{C}_{\text{ax}}\text{FeC}_{\text{eq}}\parallel$	498/494	501/496	490/486	493/487	492	489	8/8	8/9	–	9.2
A <sub>1</sub>	$\delta\text{FeCN}_{\text{eq}}\parallel, \nu\text{FeN}$	460	466	447 sh	454	460	453	13	12	7	9.6
B <sub>2</sub>	$\delta\text{FeCN}_{\text{eq}}\perp$	459	462	446	449	–	–	13	13	–	16.1
E	$\delta\text{FeCN}_{\text{eq}}\perp, \delta\text{FeCN}_{\text{ax}}$	435/432	439/435	422/418	426/421	437/434	430/424	13/14	13/14	7/10	14.1
E	$\nu\text{FeC}_{\text{eq}}, \delta\text{FeCN}_{\text{eq}}\perp$	423/417	426/419	412/408	416/410	–	–	11/9	10/9	–	10.2
B <sub>1</sub>	$\delta\text{FeCN}_{\text{eq}}$	–	417 sh	404 sh	406	–	409	–	11	–	13.2
A <sub>1</sub>	$\nu\text{FeC}_{\text{eq}}$	395 sh	399	388 sh	392	397 sh	390 sh	7	7	9	7.4
A <sub>1</sub>	$\nu\text{FeC}_{\text{ax}}$	390	391	383	384	390	384	7	7	8	6.8
E	$\delta\text{FeCN}_{\text{eq}}\parallel$	326/321	326/321	317/313	319/312	326/320	318/314	9/8	7/9	8/6	8.1
A <sub>1</sub> /E	$\delta\text{NFeC}_{\text{eq}}, \delta\text{C}_{\text{ax}}\text{FeC}_{\text{eq}}, \delta\text{C}_{\text{eq}}\text{FeC}_{\text{eq}}$	125	125	125	125	120	120	0	0	–	0.2/0.4
B <sub>2</sub>	$\delta\text{C}_{\text{eq}}\text{FeC}_{\text{eq}}$	102	103	102	103	106	106	0	0	0	0.5
B <sub>1</sub>	$\delta\text{NFeC}_{\text{eq}}$	86	91	86	91	85	85	0	0	0	0.4
E	$\delta\text{NFeC}_{\text{eq}}$	66	68	66	67	–	–	0	1	–	0.2

<sup>a</sup>Correspond to a C<sub>4v</sub> point group for the anion.<sup>b</sup>Approximate descriptions: ax, axial; eq, equatorial; angular deformations in planes parallel ( $\parallel$ ); or perpendicular ( $\perp$ ) to the C<sub>4</sub> axis.<sup>c</sup>r.t.: room temperature; l.t.: low temperature.<sup>d</sup> $\Delta_i$ : isotopic shifts.<sup>e</sup>Calculated isotopic shifts [13].

The most relevant features in the successive spectral regions are discussed below.

#### 4.1. 2200 to 1900 cm<sup>−1</sup> region

The anion should have one axial (A<sub>1</sub>) and three equatorial CN (A<sub>1</sub>, B<sub>2</sub>, E) stretching modes (the C<sub>4v</sub> symmetry species are indicated in parentheses). The corresponding bands of the isotopically normal anion are downshifted about 30 cm<sup>−1</sup> in comparison with NaNP [2].

The measured shifts after <sup>13</sup>C replacement coincide very well with the calculated values, both at room and low temperatures (Table 1). The infrared spectrum of the normal substance shows several

weak bands in the 2110–2070 cm<sup>−1</sup> region (see insert in Fig. 1), which are due to the stretching of <sup>12</sup>C<sup>15</sup>N and <sup>13</sup>C<sup>14</sup>N groups present in very low natural abundance (<sup>13</sup>C: 1.1%; <sup>15</sup>N: 0.37%) and correspond therefore to vibrationally isolated modes.

The wavenumber of these bands appears in Table 2 and the assignments are immediate with the help of simple calculations [16]. After <sup>13</sup>C replacement in TINP four intense infrared bands appear in the <sup>13</sup>C<sup>14</sup>N stretching region, as it happens with the normal substance in the <sup>12</sup>C<sup>14</sup>N region, which are accompanied by weak bands at both sides of the massif (see inserts in Fig. 1). These bands are due to the isolated <sup>12</sup>C<sup>14</sup>N, <sup>12</sup>C<sup>15</sup>N and <sup>13</sup>C<sup>15</sup>N groups. The appearance of five bands for each of the isolated groups <sup>12</sup>C<sup>14</sup>N,

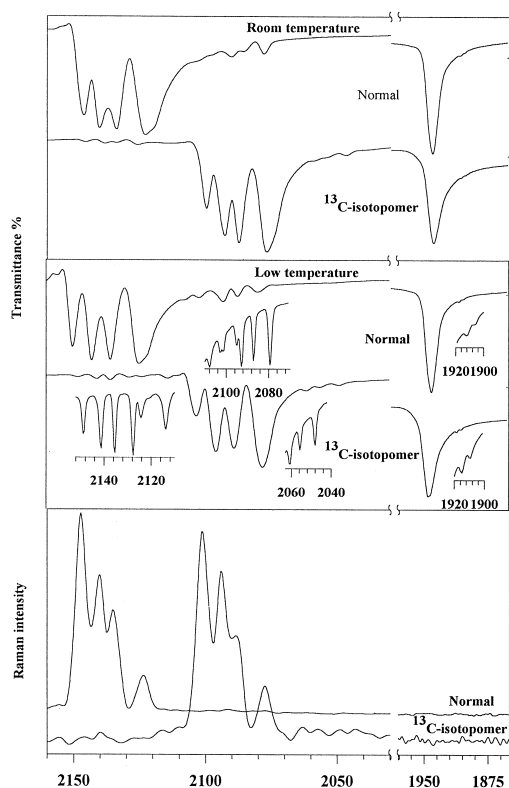


Fig. 1. Infrared and Raman spectra of  $\text{Tl}_2[\text{Fe}(\text{CN})_5\text{NO}]$  in the high wavenumbers region.

$^{12}\text{C}^{15}\text{N}$  and  $^{13}\text{C}^{14}\text{N}$  clearly corresponds with the crystallographic inequivalence of the five CN groups in  $\text{TlNP}$ , caused by the low site symmetry ( $\text{C}_1$ ).

Wavenumber differences between the stretchings of concentrated (coupled) and diluted (isolated) CN groups are not greater than  $3\text{ cm}^{-1}$ , showing that little intra- and inter-anionic interactions exist between CN groups (see Tables 1 and 2).

Bands assigned to isolated  $^{15}\text{N}^{16}\text{O}$  and  $^{14}\text{N}^{18}\text{O}$  (natural abundance of  $^{18}\text{O}$ : 0.20%) groups appear very weakly at  $1911$  and  $1905\text{ cm}^{-1}$ , respectively.

In accordance with the very low Raman intensity of the NO stretching, no Raman band was observed for this group in  $\text{TlNP}$ .

#### 4.2. 700 to $300\text{ cm}^{-1}$ region

The bands observed in this region (Fig. 2) correlate well with the corresponding bands of  $\text{NaNP}$ .

Good agreement was found between measured and calculated  $^{13}\text{C}$  shifts (Table 1).

An exception to the previous statement is the  $390\text{ cm}^{-1}$  band which, at variance with  $\text{NaNP}$ , appears in the infrared spectra outside from the complex  $450\text{--}395\text{ cm}^{-1}$  region where the corresponding  $\text{NaNP}$  band is immersed. The Raman counterpart is relatively intense, allowing their assignment to the  $\nu\text{FeC}_{\text{ax}}$  ( $\text{A}_1$  symmetry in the approximation of  $\text{C}_{4v}$  molecular point group). A relatively low wavenumber for that stretching mode was also observed for  $\text{RbNP}$  ( $392\text{ cm}^{-1}$ ) [5].

The E modes (ideal  $\text{C}_{4v}$  symmetry) appear clearly split in this spectral region for  $\text{TlNP}$ , particularly at low temperatures, as can be appreciated in Fig. 2 and detailed in Table 1. Such splitting allowed a secure assignment for such modes in  $\text{TlNP}$  and, by extension, in other nitroprussides as well.

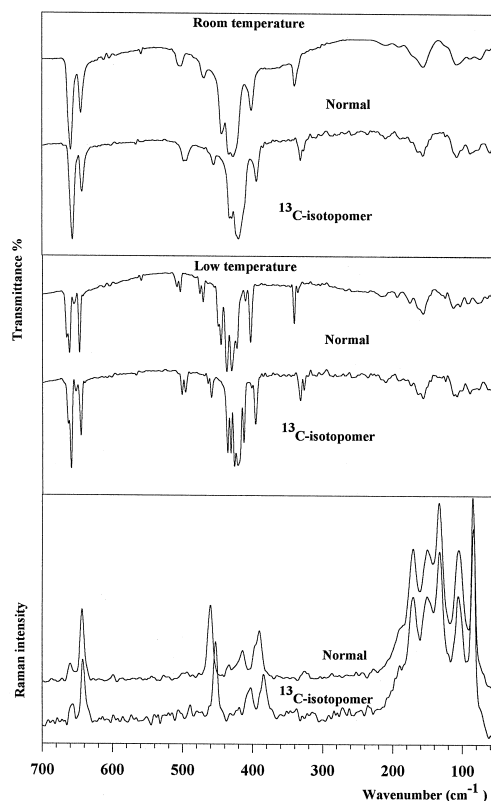


Fig. 2. Infrared and Raman spectra of  $\text{Tl}_2[\text{Fe}(\text{CN})_5\text{NO}]$  in the low wavenumbers region.

Table 2

Room temperature IR wavenumbers<sup>a</sup> of CN stretching bands of thallium nitroprusside isotopically normal and <sup>13</sup>C-enriched

Species	Assignment	<sup>12</sup> C <sup>14</sup> N	<sup>12</sup> C <sup>15</sup> N <sup>d</sup>	<sup>13</sup> C <sup>14</sup> N <sup>e</sup>	<sup>13</sup> C <sup>15</sup> N <sup>f</sup>
<sup>12</sup> C <sup>b</sup>	$\nu\text{CN}_{\text{ax}}$	2146		<b>2099</b>	
	$\nu\text{CN}_{\text{eq}}$	2140		<b>2093</b>	
	$\nu\text{CN}_{\text{eq}}$	2133	<b>2105</b>	<b>2090</b>	
	$\nu\text{CN}_{\text{eq}}$	2122	<b>2101</b>	<b>2086</b>	
	$\nu\text{CN}_{\text{eq}}$		<b>2097</b>	<b>2077</b>	
<sup>13</sup> C <sup>c</sup>	$\nu\text{CN}_{\text{ax}}$	<b>2145</b>	<b>2115</b>	2100	
	$\nu\text{CN}_{\text{eq}}$	<b>2137</b>	<b>2110</b>	2093	
	$\nu\text{CN}_{\text{eq}}$	<b>2133</b>		2087	<b>2058</b>
	$\nu\text{CN}_{\text{eq}}$	<b>2124</b>		2076	<b>2054</b>
	$\nu\text{CN}_{\text{eq}}$	<b>2113</b>			<b>2046</b>

<sup>a</sup> In bold type: wavenumbers of bands due to isolated groups.

<sup>b</sup> Isotopically normal substance.

<sup>c</sup> <sup>13</sup>C-enriched substance.

<sup>d</sup>  $\Delta_i \approx 30 \text{ cm}^{-1}$ .

<sup>e</sup>  $\Delta_i \approx 50 \text{ cm}^{-1}$ .

<sup>f</sup>  $\Delta_i \approx 80 \text{ cm}^{-1}$ .

However, the assignments are not completely clear in the 450–390  $\text{cm}^{-1}$  region. In fact, five normal modes (for the  $C_{4v}$  model) are predicted by the calculations in such a region [13],  $A_1 + B_1 + B_2 + 2E$ , whereas six bands are observed at low temperature (Table 1).

The band at 459  $\text{cm}^{-1}$ , outside that range, is assigned to the  $B_2$  mode by comparison with NaNP [13]. The above mentioned 390  $\text{cm}^{-1}$  band should be due to the  $A_1$  mode, whereas the two E modes are immediately associated to the split bands located at 435/432  $\text{cm}^{-1}$  and 423/417  $\text{cm}^{-1}$ . This leaves us with three unassigned bands in that region. The weak 395  $\text{cm}^{-1}$  band shows appreciable intensity in Raman and the expected isotopic shift, suggesting that it can have its origin in the symmetric  $\text{FeC}_{\text{eq}}$  stretching ( $A_1$ ). Therefore, one of the two remaining features (at 417sh and 412  $\text{cm}^{-1}$  in the low temperature infrared spectrum) should be assigned to the  $B_1$  mode, active in infrared because of the low anion symmetry in the crystalline lattice, although we do not have at present experimental arguments to decide between these bands.

#### 4.3. 200 to 50 $\text{cm}^{-1}$ region

In this region,  $\text{NFeC}_{\text{eq}}$ ,  $\text{C}_{\text{eq}}\text{FeC}_{\text{eq}}$  and  $\text{C}_{\text{ax}}\text{FeC}_{\text{eq}}$  bending bands and lattice modes appear. Raman

spectra are more helpful in this region than the infrared spectra due to the higher intensity and better definition of bands. As stated above, assignment of bands attributed to the anion follows a previous study of NaNP [13]. See Table 1 for infrared and Raman wavenumbers and assignments.

## 5. Overtone and combinations bands

Numerous infrared overtone (up to the third for the NO stretching) and combination bands have been observed for <sup>12</sup>C- and <sup>13</sup>C-TINP. The measured infrared spectra are reproduced in Figs. 3 and 4, while the wavenumbers of the observed features as well as the corresponding assignments appear in Table 3.

No reference was found in the literature about the near infrared (NIR) spectrum of nitroprussides. The NIR spectrum of TINP is considerably simpler than the equivalent spectrum of hydrated NaNP, because in this last case numerous overtone and combination bands of the hydration water molecules appear in the 8000–4000  $\text{cm}^{-1}$  region [14].

### 5.1. NO overtones and anharmonicity constant

The very strong infrared NO stretching band appears at 1947  $\text{cm}^{-1}$  in the room temperature infrared spectrum of the isotopically normal substance and its first three overtones appear at 3871, 5764 and 7635  $\text{cm}^{-1}$ , respectively (see Table 3 and Fig. 3). This data allowed the calculation of the anharmonicity

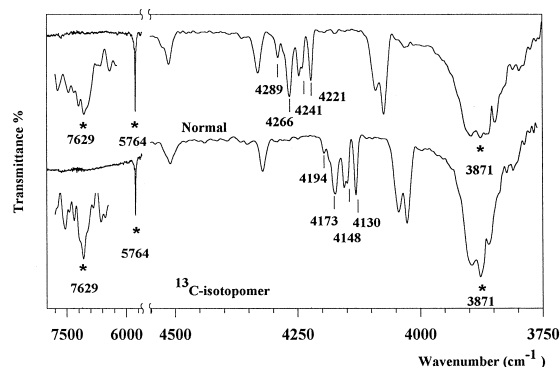


Fig. 3. Overtone and combination bands of  $\text{Tl}_2[\text{Fe}(\text{CN})_5\text{NO}]$  in the near infrared. The overtones of the NO stretching vibration are indicated with asterisks.

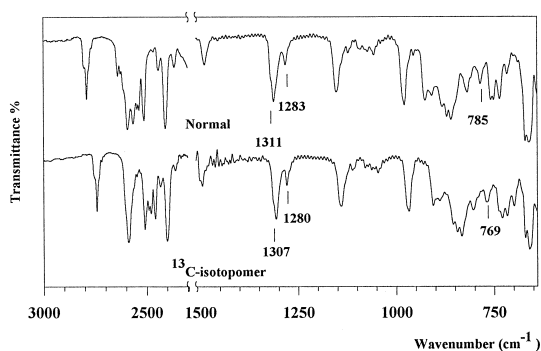


Fig. 4. Overtone and combination bands of  $\text{Ti}_2[\text{Fe}(\text{CN})_5\text{NO}]$  in the medium infrared.

constant ( $\tilde{\omega}_e x_e$ ) and harmonic stretching wavenumber ( $\tilde{\omega}_e$ ) of the NO group. Considering NO as a diatomic anharmonic oscillator, observed wavenumbers,  $\tilde{\nu}_n$ , for the fundamental ( $n = 1$ ) and the overtones ( $n = 2-4$ ), should fit the following equation in a first approximation [17]:  $\tilde{\nu}_n/n = \tilde{\omega}_e - \tilde{\omega}_e x_e(n + 1)$ . Least squares fitting of observed wavenumbers results in the following equation:  $\tilde{\nu}_n/n = 1959 - 12.68(n + 1)$ . The obtained anharmonicity constant,  $\tilde{\omega}_e x_e = 12.68 \text{ cm}^{-1}$  is higher than in sodium nitroprusside dihydrate:  $10.2 \text{ cm}^{-1}$  for ( $^{14}\text{N}^{16}\text{O}$ ) and  $9.07 \text{ cm}^{-1}$  for ( $^{15}\text{N}^{16}\text{O}$ ) [18].

## 5.2. Bands involving CN stretchings

CN stretchings overtone and combination bands appear in two regions:  $4300$  to  $4000 \text{ cm}^{-1}$  (Fig. 3) and  $2800$  to  $2500 \text{ cm}^{-1}$  (Fig. 4). The first region includes three overtones and three combinations, and of these latter, one is between CN stretchings, which shifts isotopically  $93 \text{ cm}^{-1}$ , and two, between a different CN stretching in each case and  $\nu\text{NO}$ , which shift around  $47 \text{ cm}^{-1}$ . The band at  $4221$  ( $^{12}\text{C}$ )/ $4130$  ( $^{13}\text{C}$ )  $\text{cm}^{-1}$  can be explained as the first overtone of a component of the broad  $2122 \text{ cm}^{-1}$  band, centered at about  $2113 \text{ cm}^{-1}$ ; the isotopic shift is in accordance with such assignment.

In the second region, from  $2800$  to  $2500 \text{ cm}^{-1}$  (Fig. 4), the observed bands can be assigned to combinations of  $\nu\text{CN}$  with  $\delta\text{FeNO}$ ,  $\delta\text{FeCN}$  and  $\nu\text{FeC}$ , which downshift  $49-58 \text{ cm}^{-1}$ . Also, the combination band  $\nu\text{NO} + \delta\text{FeNO}$  is observed in this region at  $2592 \text{ cm}^{-1}$ ; this band shifts  $4 \text{ cm}^{-1}$  upon  $^{13}\text{C}$  substitution.

In the region comprised between  $1500$  to  $700 \text{ cm}^{-1}$ , bands due to the first overtones of  $\delta\text{FeNO}$  and  $\nu\text{FeN}$  (second overtones are surely overlapped by the strong  $\nu\text{NO}$  fundamental band) and to combinations of fundamentals are present.

Table 3

Wavenumbers and isotopic shifts of overtone and combination bands and the corresponding assignments in the near and medium infrared regions

$^{12}\text{C}^a$	$^{13}\text{C}^b$	$\Delta_i^c$	Assignment	$\Delta_i^d$
7629	7629	12	$1947 \times 4 = 7788$	$2 \times 4 = 8$
5764	5764	0	$1947 \times 3 = 5841$	$2 \times 3 = 6$
4513	4509	4	$2 \times 1947 + 643 = 4537$	$4 + 2 = 6$
4331	4322	9	$2 \times 1947 + 460 = 4354$	$4 + 13 = 17$
4289	4194	95	$2146 \times 2 = 4292$	$47 \times 2 = 94$
4266	4173	93	$2134 \times 2 = 4268$	$46 \times 2 = 92$
4247	4154	93	$2134 + 2123 = 4257$	$47 + 46 = 93$
4241	4148	93	$2122 \times 2 = 4244$	$46 \times 2 = 92$
4221	4130	91	ca. $2113 \times 2 = 4226$	$46 \times 2 = 92$
4090	4044	46	$2146 + 1947 = 4093$	$47 + 2 = 49$
4075	4027	48	$2134 + 1947 = 4081$	$47 + 2 = 49$
3871	3871	1	$1947 \times 2 = 3894$	$2 \times 2 = 4$
2800	2750	50	$2146 + 659 = 2805$	$47 + 3 = 50$
2790	2741	49	$2140 + 659 = 2799$	$47 + 3 = 50$
2639	<sup>e</sup>	<sup>e</sup>	$2146 + 496 = 2642$	$47 + 8 = 55$
2626	<sup>e</sup>	<sup>e</sup>	$2140 + 496 = 2636$	$47 + 8 = 55$
2613	<sup>e</sup>	<sup>e</sup>	$2122 + 496 = 2618$	$46 + 8 = 54$
2592	2588	4	$1947 + 659 = 2606$	$2 + 3 = 5$
2563	2508	55	$2134 + 434 = 2568$	$47 + 14 = 61$
2546	2488	58	$2134 + 420 = 2554$	$47 + 10 = 57$
2536	2478	58	$2122 + 420 = 2542$	$46 + 10 = 56$
2512	2458	54	$2122 + 390 = 2512$	$46 + 7 = 53$
2408	2400	8	$1947 + 496 = 2443$	$2 + 8 = 10$
1489	1493	-4	?	
1311	1307	4	$659 \times 2 = 1318$	$3 \times 2 = 6$
1283	1280	3	$643 \times 2 = 1286$	$2 \times 2 = 4$
1151	1142	9	$659 + 496 = 1155$	$3 + 8 = 11$
979	968	11	$659 + 324 = 983$	$3 + 9 = 12$
926	906	20	$496 + 434 = 930$	$8 + 14 = 22$
910	889	21	$460 + 459 = 919$	$13 + 13 = 26$
882	854	28	$459 + 434 = 893$	$13 + 13 = 26$
871	844	27	$460 + 420 = 880$	$13 + 10 = 23$
861	833	28	$459 + 420 = 879$	$13 + 10 = 23$
820	803	17	$434 + 390 = 824$	$14 + 7 = 21$
785	769	16	$395 \times 2 = 790$	$7 \times 2 = 14$
751	729	22	$324 + 434 = 758$	$9 + 14 = 23$
736	716	20	$324 + 420 = 744$	$9 + 10 = 19$
716	700	16	$324 + 395 = 719$	$9 + 7 = 16$

<sup>a</sup> Isotopically normal substance.

<sup>b</sup>  $^{13}\text{C}$ -enriched substance.

<sup>c</sup> Isotopic shift  $^{12}/^{13}\text{C}$ .

<sup>d</sup> Isotopic shifts combinations.

<sup>e</sup>  $^{13}\text{C}$ -shifted band lies under the broad band located at  $2588 \text{ cm}^{-1}$ .

The anharmonicity constant calculated from fundamental and first overtone bands for  $\delta\text{FeNO}$  and  $\nu\text{FeN}$  are 4.5 and 1.5  $\text{cm}^{-1}$  and the corresponding  $\tilde{\omega}_e$  values are 668 and 646  $\text{cm}^{-1}$ , respectively.

## 6. Lattice modes

Fifteen restricted translational ( $10A' + 5A''$ ) and six ( $2A' + 4A''$ ) rotational (librational) optical lattice modes, all infrared and Raman active, are expected. Infrared and Raman wavenumbers for  $^{12}\text{C}$  and  $^{13}\text{C}$  isotopomers of TINP in the lattice modes region are presented in Table 4. Only a few isotopic shifts could be measured in the infrared spectra, mainly at low temperature.

The bands which suffer isotopic shifts greater than 1  $\text{cm}^{-1}$  could be assigned in principle to librational modes, which present larger shifts than translational modes [19]. The other bands could be due, therefore, to these translational modes.

Trying to confirm those assignments, and taking into account that a change of the nature of the cation should affect much more the translational than the librational modes [19], data about lattice modes of TINP and other anhydrous nitroprussides of monovalent cations, i.e., RbNP, CsNP and TBANP are compared in Table 5. NaNP (dihydrate) are also included in Table 5. Unfortunately, data are not complete and shifts, when occurring, are small and sometimes erratic. Only the band at 139–133  $\text{cm}^{-1}$

Table 5

Infrared and Raman lattice modes observed for sodium nitroprusside dihydrate and anhydrous rubidium, cesium, thallium and tetrabutylammonium nitroprussides<sup>a</sup>

Na [2]		Rb [5]		Cs [6]		Tl <sup>b</sup>		TBA <sup>b</sup>	
IR	R	IR	R	IR	R	IR	R	IR	R
190	–	–	–	–	–	191	190	202	–
–	164	–	168	–	–	172	171	–	–
–	158	–	–	–	–	–	–	–	–
147	–	–	147	–	145	151	151	150	149
139	136	–	136	–	133	135	133	135	–
116	–	–	–	–	–	–	–	–	–
–	–	–	–	–	–	78	–	77	–

<sup>a</sup>Wavenumbers. Room temperature data.

<sup>b</sup>This work.

seems to decrease slightly in wavenumber with increasing mass of the cation.

## 7. Summary and conclusions

TINP, which is one of the few nitroprussides that crystallize anhydrous, presents an infrared spectrum obviously not complicated by water bands. This fact, together with splittings of otherwise degenerated bands due mainly to site symmetry effect and band shifts produced by  $^{13}\text{C}$  substitution facilitate the interpretation of the spectral features. External (lattice) vibrational behaviour is much less clear. Isotopic shifts were helpful for the assignment of fundamental modes, overtones and combinations but not for lattice modes. The overtones of the FeNO grouping vibrations allowed the calculation of the corresponding anharmonicity constants. The value of such constant for the NO stretching is in accordance with previous results obtained with sodium nitroprusside dihydrate [18].

## Acknowledgements

To CONICET and CICPBA for financial help received through CEQUINOR; to CONICET, for the grant PIP#4752, to ANPCYT for the grant PICT#06-00005-00118, and to UNLP, for support as part of a research incentive program.

Table 4

Infrared spectra of isotopic  $^{12/13}\text{C}$  shifts ( $\Delta_i$ ) at room (r.t.) and low temperature (l.t.) and Raman (r.t.) for lattice modes of TINP. Units are  $\text{cm}^{-1}$ <sup>a</sup>

Infrared				Raman		$\Delta_i$ $^{12/13}\text{C}$ ( $\text{cm}^{-1}$ )		
$^{12}\text{C}$ r.t.	$^{12}\text{C}$ l.t.	$^{13}\text{C}$ r.t.	$^{13}\text{C}$ l.t.	$^{12}\text{C}$	$^{13}\text{C}$	IR r.t.	IR l.t.	Raman
191	196	191	191	190	190	0	5	0
172	175	170	172	171	171	2	3	0
151	155	151	154	151	151	0	1	0
135	136	134	136	133	133	1	0	0
91	94	91	91	–	–	0	3	–
77	81	78	78	–	–	1	3	–
53	54	53	53	–	–	0	1	–
39	41	39	40	–	–	0	1	–

<sup>a</sup>For tentative assignments see text.



## References

- [1] M.M. Vergara, E.L. Varetto, *Spectrochim. Acta* 49A (1993) 527.
- [2] M.E. Chacón Villalba, E.L. Varetto, P.J. Aymonino, *Vib. Spectrosc.* 14 (1997) 275.
- [3] J.I. Amalvy, E.L. Varetto, P.J. Aymonino, E.E. Castellano, O.E. Piro, G. Punte, *J. Crystallogr. Spectrosc. Res.* 16 (1986) 537.
- [4] J.I. Amalvy, E.L. Varetto, P.J. Aymonino, *J. Phys. Chem. Solids* 46 (1985) 1153.
- [5] D.B. Soria, J.I. Amalvy, O.E. Piro, E.E. Castellano, P.J. Aymonino, *J. Chem. Crystallogr.* 26 (1996) 325.
- [6] M.M. Vergara, E.L. Varetto, G. Rigotti, A. Navaza, *J. Phys. Chem. Solids* 50 (1989) 951.
- [7] J.I. Amalvy, E.L. Varetto, P.J. Aymonino, *An. Asoc. Quim. Argent.* 74 (1986) 437.
- [8] G. Rigotti, P.J. Aymonino, E.L. Varetto, *J. Crystallogr. Spectrosc. Res.* 14 (1984) 517.
- [9] C.O. Della Védova, J.H. Lesk, E.L. Varetto, P.J. Aymonino, *J. Mol. Struct.* 70 (1981) 241.
- [10] O.E. Piro, S.R. González, P.J. Aymonino, *Phys. Rev.* 36 (1987) 3125.
- [11] A. Benavente, J.A. de Morán, O.E. Piro, E.E. Castellano, P.J. Aymonino, *J. Chem. Crystallogr.* 27 (1997) 343.
- [12] G. Rigotti, G. Punte, B.E. Rivero, E.E. Castellano, *Acta Crystallogr. B* 36 (1980) 1475.
- [13] M.E. Chacón Villalba, E.L. Varetto, P.J. Aymonino, *Spectrochim. Acta* 55A (1999) 1545.
- [14] M.E. Chacón Villalba, E.L. Varetto, P.J. Aymonino, XX Congreso Argentino de Química, Córdoba, R. Argentina, 1994.
- [15] G. Rigotti, Doctoral Thesis, Facultad de Ciencias Exactas, Universidad Nacional de La Plata, 1980.
- [16] M.E. Chacón Villalba, E.L. Varetto, P.J. Aymonino, *Vib. Spectrosc.* 4 (1992) 109.
- [17] G. Herzberg, *Molecular Spectra and Molecular Structure I, Diatomic Molecules*, Van Nostrand, New York, 1945.
- [18] M.E. Chacón Villalba, E.L. Varetto, P.J. Aymonino, IX Congreso Argentino de Fisicoquímica, San Luis, R. Argentina, 1994.
- [19] P.M.A. Sherwood, *Vibrational Spectroscopy of Solids*, Cambridge Univ. Press, Cambridge, 1972.